Article

Single-Conformation Ultraviolet and Infrared Spectroscopy of Model Synthetic Foldamers: β-Peptides Ac-β-hPhe-β-hAla-NHMe and Ac-β-hAla-β-hPhe-NHMe

Esteban E. Baquero, William H. James, Soo Hyuk Choi, Samuel H. Gellman, and Timothy S. Zwier

J. Am. Chem. Soc., **2008**, 130 (14), 4795-4807 • DOI: 10.1021/ja078272q

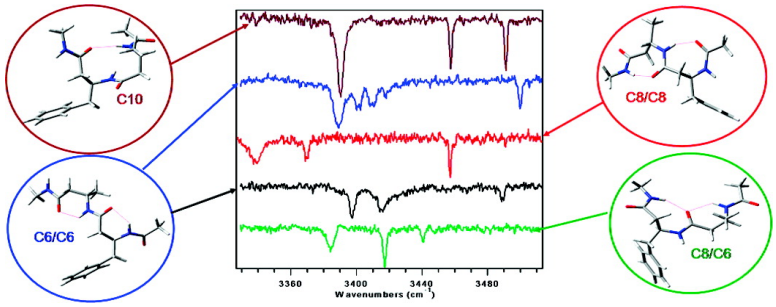

More About This Article

Additional resources and features associated with this article are available within the HTML version:

- Supporting Information
- Links to the 4 articles that cite this article, as of the time of this article download
- Access to high resolution figures
- Links to articles and content related to this article
- Copyright permission to reproduce figures and/or text from this article

View the Full Text HTML

J|A|C|S
ARTICLES
Published on Web 03/18/2008

Single-Conformation Ultraviolet and Infrared Spectroscopy of Model Synthetic Foldamers: β-Peptides Ac-β^3-hPhe-β^3-hAla-NHMe and Ac-β^3-hAla-β^3-hPhe-NHMe

Esteban E. Baquero,[‡] William H. James III,[‡] Soo Hyuk Choi,[#] Samuel H. Gellman,[#] and Timothy S. Zwier*[,‡]

Department of Chemistry, Purdue University, West Lafayette, Indiana 47907-2084, and Department of Chemistry, University of Wisconsin, Madison, Wisconsin 53706-1322

Received October 29, 2007; E-mail: zwier@purdue.edu

Abstract: The conformational preferences and infrared and ultraviolet spectral signatures of two model β-peptides, Ac-β^3-hPhe-β^3-hAla-NHMe (**1**) and Ac-β^3-hAla-β^3-hPhe-NHMe (**2**), have been explored under jet-cooled, isolated-molecule conditions. The mass-resolved, resonant two-photon ionization spectra of the two molecules were recorded in the region of the S_0-S_1 origin of the phenyl substituents (37200−37800 cm^{-1}). UV−UV hole-burning spectroscopy was used to determine the ultraviolet spectral signatures of five conformational isomers of both **1** and **2**. Transitions due to two conformers (labeled A and B) dominate the R2PI spectra of each molecule, while the other three are minor conformers (C−E) with transitions a factor of 3−5 smaller. Resonant ion-dip infrared spectroscopy was used to obtain single-conformation infrared spectra in the 3300−3700 cm^{-1} region. The infrared spectra showed patterns of NH stretch transitions characteristic of the number and type of intramolecular H-bonds present in the β-peptide backbone. For comparison with experiment, full optimizations of low-lying minima of both molecules were carried out at DFT B3LYP/6-31+G*, followed by single point MP2/6-31+G* and selected MP2/aug-cc-pVDZ calculations at the DFT optimized geometries. Calculated harmonic vibrational frequencies and infrared intensities for the amide NH stretch vibrations were used to determine the β-peptide backbone structures for nine of the ten observed conformers. Conformers **1B**, **1D**, and **2A** were assigned to double ring structures containing two C6 H-bonded rings (C6a/C6a), conformers **1A** and **2B** are C10 single H-bonded rings, conformers **1C** and **2D** are double ring structures composed of two C8 H-bonded rings (C8/C8), and conformers **1E** and **2E** are double ring/double acceptor structures in which two NH groups H-bond to the same C═O group, thereby weakening both H-bonds. Both **1E** and **2E** are tentatively assigned to C6/C8 double ring/double acceptor structures, although C8/C12 structures cannot be ruled out unequivocally. Finally, no firm conformational assignment has been made for conformer **2C** whose unusual infrared spectrum contains one very strong H-bond with NH stretch frequency at 3309 cm^{-1}, a second H-bonded NH stretch fundamental of more typical value (3399 cm^{-1}), and a third fundamental at 3440 cm^{-1}, below that typical of a branched-chain free NH. The single conformation spectra provide characteristic wavenumber ranges for the amide NH stretch fundamentals ascribed to C6 (3378−3415 cm^{-1}), C8 (3339−3369 cm^{-1}), and C10 (3381−3390 cm^{-1}) H-bonded rings.

1. Introduction

β-Peptides are synthetic foldamers[1−4] in which two carbons separate adjacent amide groups rather than the single carbon atom present in naturally occurring α-peptides. In the first paper of this series,[5] we reported the ultraviolet and infrared spectroscopy of single conformations of two model β-peptides, 3-acetoamido-*N*-methyl-4-phenylbutamide (Ac-β^3-hPhe-NHMe, Figure 1a, **3**) and 3-acetamido-4-(-hydroxyphenyl)-*N*-methylbutamide (Ac-β^3-hTyr-NHMe, Figure 1b, **4**). The gas-phase, jet-cooled spectra of these molecules were dominated by a single conformation assignable based on its amide NH stretch infrared spectrum to a structure containing a six-membered ring H-bond, labeled as C6. A second, very weak transition in **3** was also observed and assigned based on its infrared spectrum to a structure containing a C8 H-bonded ring with an unusually weak C8 H-bond. A key to these assignments was the recognition that the two amide NH groups have unique spectral signatures in the absence of an intramolecular H-bond, with the C-terminal NH, which is bonded to a methyl group, appearing at 3488 cm^{-1}, while the interior NH, which is bonded to a branched-chain carbon atom, appears at 3454 cm^{-1}.

In paper II of this series, we extend these studies of β-peptides to include Ac-β^3-hPhe-β^3-hAla-NHMe (Figure 1c, **1**) and Ac-

[‡] Purdue University.
[#] University of Wisconsin.

(1) Cheng, R. P.; Gellman, S. H.; DeGrado, W. F. *Chem. Rev.* **2001**, *101*, 3219−3232.
(2) Dado, G. P.; Gellman, S. H. *J. Am. Chem. Soc.* **1994**, *116*, 1054−1062.
(3) Seebach, D.; Beck, A. K.; Bierbaum, D. J. *Chem. Biodivers.* **2004**, *1*, 1111−1239.
(4) Seebach, D.; Matthews, J. L. *Chem. Commun.* **1997**, 2015−2022.
(5) Baquero, E. E.; James, W. H.; Choi, S. H.; Gellman, S. H.; Zwier, T. S. *J. Am. Chem. Soc.* **2008**, *130*, 4784−4794.

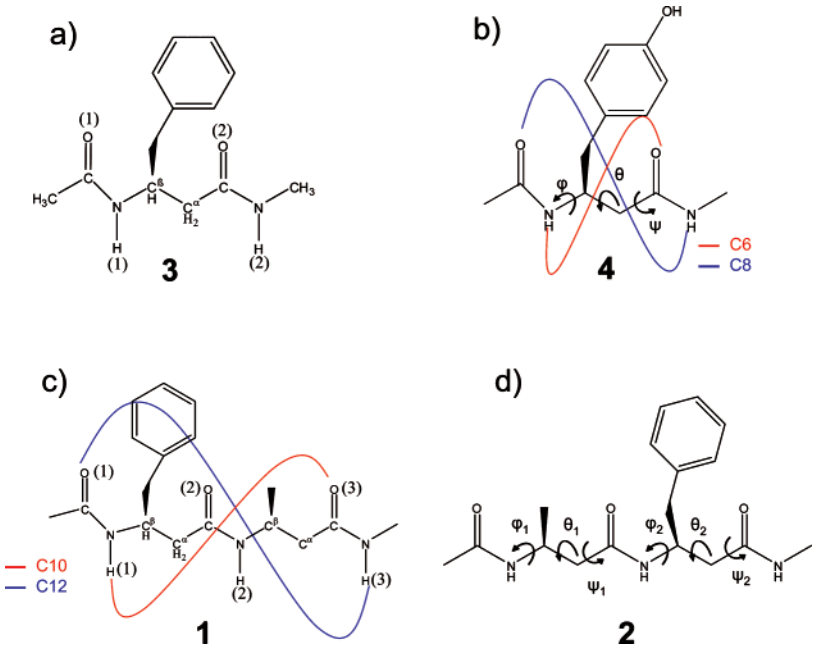

Figure 1. Structures for (a) 3-acetoamido-*N*-methyl-4-phenylbutamide (Ac-β^3-hPhe-NHMe, **3**) and (b) 3 acetamido-4-(-hydroxyphenyl)-*N*-methylbutamide (Ac-β^3-hTyr-NHMe, **4**), reported in the preceding paper in this issue.[5] Structures for (c) Ac-β^3-hPhe-β^3-hAla-NHMe (**1**) and (d) Ac-β^3-hAla-β^3-hPhe-NHMe (**2**). Structures in a and c show the labeling scheme for amide groups along the peptide chains. Structures shown in b and d show the relevant Ramachandran angles associated with β-peptide conformational search. The solid lines in b and c show possible intramolecular hydrogen bonded interactions that form C*n* rings, where '*n*' is the number of atoms in the H-bonded ring formed.

β^3-hAla-β^3-hPhe-NHMe (Figure 1d, **2**). These molecules differ from **3** by addition of another β-amino acid residue to the backbone, thereby greatly increasing the conformational possibilities. Now, in addition to the single ring C6 structures, C6/C6 and C8/C8 double rings are possible, as are larger C10 and C12 single rings, and unusual double ring/double acceptor structures (C6/C8 and C8/C12) in which two NH groups H-bond to the same carbonyl group. Since these prototypical H-bonded conformations are important sub-elements of larger secondary structures (e.g., helices and sheets), it is important to determine their spectral signatures for comparison with solution-phase work and to provide benchmark data for comparison with *ab initio* and density functional theory methods. The observed conformational preferences can also be used by those developing molecular mechanics force fields.

In this paper, we present resonant two-photon ionization (R2PI), UV−UV hole-burning, and resonant ion-dip infrared (RIDIR) spectra for **1** and **2**. A total of ten conformational isomers are distinguished and spectroscopically characterized, five in **1** and five in **2**. We shall see that the experimental spectra display representatives of all the above-mentioned H-bonding architectures, providing a rich data set that contains fundamental insight to the spectral signatures associated with each. Single ring and double ring structures are easily distinguished from one another based on the number of H-bonded NH stretch fundamentals. The distinct frequencies of the terminal and interior free NH stretch transitions further constrain the possibilities.[6] Finally, comparison with Becke3LYP density functional method[7,8] calculations provides firm assignments for nine of the ten observed conformers.

(6) Marraud, M.; Neel, J. *J. Polym. Sci. Part C: Polym. Symp.* **1975**, *52*, 271−282.
(7) Becke, A. D. *J. Chem. Phys.* **1993**, *98*, 5648−5652.
(8) Lee, C. T.; Yang, W. T.; Parr, R. G. *Phys. Rev. B* **1988**, *37*, 785.

2. Experimental Section

The preparation of *N*-Boc protected β-amino acid methyl amides and the conversion of the *N*-Boc group to the *N*-Ac group were performed as described in the adjoining publication.[5] *N*-Boc protected β^3-amino acids were purchased from Sigma-Aldrich and Chem-Impex International.

For the synthesis of Ac-β^3-hPhe-β^3-hAla-NHMe (**1**), Boc-β^3-hAla-NHMe was treated with 4.0 M HCl in dioxane solution for 1 h. After evaporation of solvent, the hydrochloride salt was dissolved in DMF. Boc-β^3-hPhe-OH (1 equiv), (*N*,*N*-dimethylamino)propyl-3-ethylcarbodiimide hydrochloride (1.5 equiv), and 4-(*N*,*N*-dimethylamino)pyridine (1.2 equiv) were added. The reaction mixture was stirred for 2 d, and water was added until a precipitate formed. Boc-β^3-hPhe-β^3-hAla-NHMe was collected by suction filtration. Deprotection of the *N*-Boc group and subsequent acetylation gave the crude product as a precipitate, which was further purified by recrystallization from a methanol/ether/*n*−heptane mixture: ^{1}H NMR (300 MHz, CD_3OD) δ 7.31−7.15 (m, 5H), 4.39 (quintet, 7.0 Hz, 1H), 4.22 (sextet, 6.8 Hz, 1H), 2.80 (ABX, J_{AB} = 13.7 Hz, J_{AX} = 6.1 Hz, J_{BX} = 8.3 Hz, $\Delta\upsilon$ = 0.08 ppm, 2H), 2.69 (s, 3H), 2.44−2.21 (m, 4H), 1.84 (s, 3H), 1.15 (d, J = 6.2 Hz); ESI-TOF MS 320.5 $[M + H]^+$, 342.5 $[M + Na]^+$, 639.9 $[2M + H]^+$, 661.9 $[2M + Na]^+$, 981.4 $[3M + Na]^+$.

Ac-β^3-hAla-β^3-hPhe-NHMe (**2**) was prepared from Boc-β^3-hPhe-NHMe and Boc-β^3-hAla-OH by a procedure analogous to that described above: ^{1}H NMR (300 MHz, CD_3OD) δ δ 7.31−7.13 (m, 5H), 4.44 (quintet, 7.0 Hz, 1H), 4.11 (sextet, 7.1 Hz, 1H), 2.81 (ABX, J_{AB} = 14.1 Hz, J_{AX} = 6.1 Hz, J_{BX} = 8.5 Hz, $\Delta\upsilon$ = 0.07 ppm, 2H), 2.69 (s, 3H), 2.44−2.29 (m, 3H), 2.11 (dd, J = 13.9, 7.4 Hz, 1H), 1.88 (s, 3H), 1.01 (d, J = 6.9 Hz); ESI-TOF MS 320.5 $[M + H]^+$, 342.5 $[M + Na]^+$, 662.0 $[2M + Na]^+$, 981.5 $[3M + Na]^+$.

The experimental apparatus and methods used in the present study to record single-conformation spectra are identical to those detailed in the preceding paper in this issue.[5] Ac-β^3-hPhe-β^3-hAla-NHMe and Ac-β^3-hAla-β^3-hPhe-NHMe were heated to 235 °C in order to obtain a sufficient vapor pressure for study by our methods. Vapor from the heated samples was entrained in a 70/30 neon/helium carrier gas at a

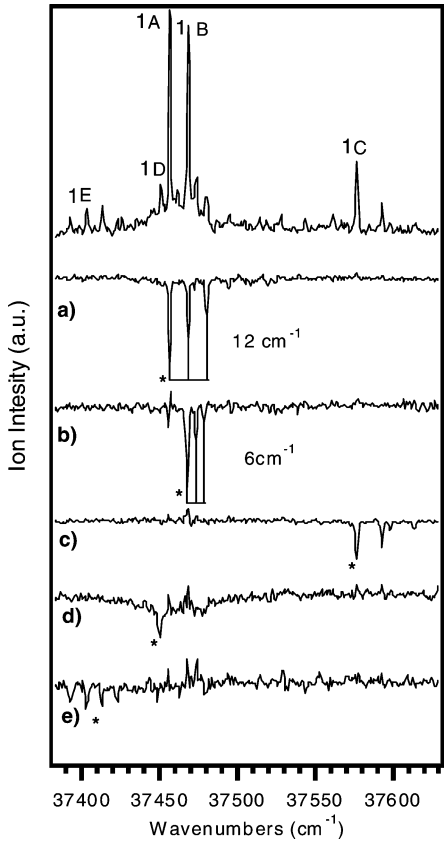

Figure 2. Top trace: R2PI spectrum of Ac-β^3-hPhe-β^3-hAla-NHMe (**1**). (a−e): UV hole-burning spectra of conformers 1A−E, respectively. The asterisks denote the transitions used as the hole-burn transition in each case.

backing pressure of 1.7 bar and expanded into vacuum through a pulsed valve. The higher temperatures used in the present work led to greater thermal decomposition of the sample than in the adjoining publication.[5] Transitions due to these decomposition products appeared at lower masses in the time-of-flight mass spectrum and so did not interfere with the present study. The dominant decomposition products appeared at *m*/*z* 260 in 1 and *m*/*z* 176 in 2, associated with breaking the N−C(β^3) bond attached to the Phe side chain.

3. Results and Analysis

3.1. Conformation Specific Spectroscopy. 3.1.1. Ac-β^3-hPhe-β^3-hAla-NHMe (1). The top trace in Figure 2 shows the resonant two photon ionization (R2PI) spectrum of Ac-β^3-hPhe-β^3-hAla-NHMe (**1**) in the S_0-S_1 origin region (37380−37640 cm^{-1}). The spectrum is dominated by two large bands at 37457 cm^{-1} (labeled **A**) and 37469 cm^{-1} (labeled **B**). The UVHB spectrum of transition **A** (Figure 2a) shows this band to be the S_0-S_1 origin for conformer **1A**, which also possesses a short Franck−Condon progression with a spacing of 12 cm^{-1}. The second band in this progression is partially overlapped with the S_0-S_1 origin of conformer **1B**. UV hole-burning indicates that conformer **1B** also possesses a progression in a low-frequency mode with a 6 cm^{-1} spacing (Figure 2b). UVHB was also carried out on several other small transitions in the spectrum (Figure 2c−e). These spectra identified transitions due to three other conformers (**1C**−**E**) with S_0-S_1origins spread over about 180 cm^{-1}. These results are summarized in Table 1.

In order to learn more about the types of structures responsible for these five conformers, resonant ion-dip infrared (RIDIR) spectra were recorded in the amide NH stretch region (3280−3530 cm^{-1}). The spectra for conformers **1A**−**E** are shown in Figure 3a−e, respectively, while the transition frequencies are summarized in Table 1. Since **1** contains three amide groups, we anticipate observing three NH stretch fundamentals for each conformer. In referring to various structures, it will be convenient to designate the three amide groups by their position along the β-peptide chain, numbering them 1−3 starting from the N-terminus to the C-terminus, as shown in Figure 1. The frequencies, intensities, and overall pattern of the RIDIR spectra reveal much about the conformational family to which each conformer belongs. Like the shorter β-peptides studied in the first paper,[5] the C-terminal amide group is methyl-capped and hence is anticipated to have a free amide NH stretch transition near 3490 cm^{-1}, while the other two NH groups are attached to branched chain carbon atoms that should be shifted to lower frequency by 30−40 cm^{-1}. As a result, the position of the free amide NH stretch transitions indicates the position of the NH

Table 1. Experimentally Determined $S_1 \leftarrow S_0$ Origins and IR Bands of the Five Conformers of Ac-β^3-hPhe-β^3-hAla-NHMe (**1**) and Ac-β^3-hAla-β^3-hPhe-NHMe (**2**)

H-bonding[a] structure	conformer[b]	$S_1 \leftarrow S_0$ origin (cm^{-1})	H-bonded N–H stretches (cm^{-1})	free branched NH (cm^{-1})	free methyl-capped NH (cm^{-1})
C6/C6	1B	37469	3388/3401	–	3500
	1D	37451	3397/3415	–	3489
	2A	37458	3378/3398	–	3490
C8/C8	1C	37577	3339/3369	3457	–
	2D	37533	3348/3367	3452	–
C10	1A	37457	3390	3457	3491
	2B	37583	3381	3447	3481
C6/C8	1E	37393	3384/3417	3440	–
	2E	37572	3366/3409	3471	–
?	2C	37552	3309/3399	3444	–

[a] Structure predicted by observation of the free and H-bonded NH stretch bands. [b] Conformers of Ac-β^3-hPhe-β^3-hAla-NHMe are labeled by 1 and Ac-β^3-hAla-β^3-hPhe-NHMe are labeled by 2.

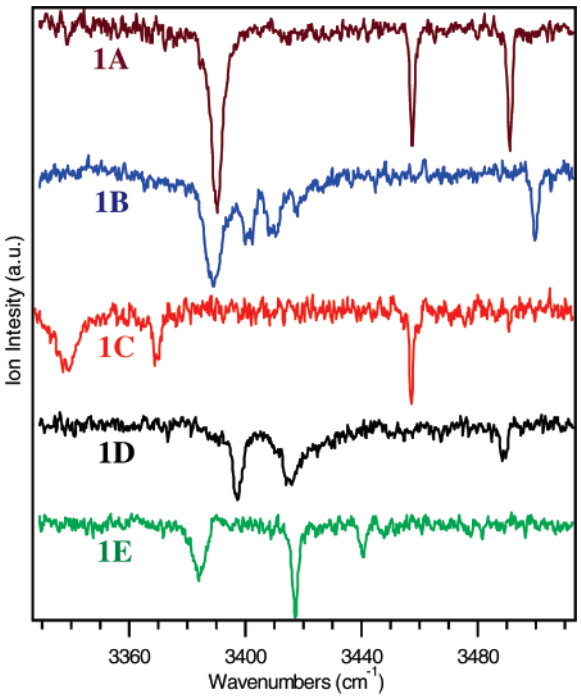

Figure 3. RIDIR spectra in the amide NH stretch region of conformers 1A−E of Ac-β^3-hPhe-β^3-hAla-NHMe (**1**).

groups that are *not* involved in H-bonds. In addition, all conformers possess at least one NH stretch fundamental that is shifted well down in frequency, signaling that the NH group responsible for the absorption is involved in a H-bond with a carbonyl group from another amide subunit. Most of these bands are also broadened and have a large integrated intensity, additional indicators of intrachain hydrogen bonding.

The RIDIR spectrum of conformer **1A** (Figure 3a) shows one H-bonded NH stretch transition at 3390 cm^{-1} and two free NH stretches at 3490 and 3457 cm^{-1} due to a methyl-terminated NH(3) and interior NH group (NH(1) or NH(2)), respectively. This set of criteria can be met in three ways. By forming a single H-bond between NH(1) and C═O(3), a 10-membered H-bonded ring results (C10, Figure 1c), leaving NH(2) and NH-(3) free. Alternatively, formation of an NH(2) → C═O(3) H-bond will form a C6 ring, leaving NH(1) and NH(3) free. Finally, an NH(1) → C═O(2) H-bond forms a C6 ring, leaving NH(2) and NH(3) free. We will see shortly that of these three, the first is by far most likely.

Conformers **1B**−**D** each possess two hydrogen bonded and one free NH stretch fundamental (Figure 3b−d), consistent with double ring structures. Conformers **1B** and **1D** have both their hydrogen-bonded fundamentals in the 3380−3420 cm^{-1} region, indicating that the two H-bonds are of similar type and strength, and free NH stretch fundamentals around 3490 cm^{-1}, indicative of a methyl-capped free NH(3). This pattern can only be satisfied by a C6/C6 double ring structure in which intrachain H-bonds are formed between NH(1) → C═O(2) and NH(2) → C═O(3), leaving NH(3) free (Figure 1c).

In contrast, conformer **1C** (Figure 3c) has its two H-bonded NH stretch fundamentals at 3328 and 3370 cm^{-1}, again pointing to two H-bonds of similar strength and type but shifted about 50 cm^{-1} below that in **1B** and **1D**. The free NH fundamental is at 3457 cm^{-1}, consistent with the free amide NH being adjacent to a branched-chain carbon. This combination of transitions can only be satisfied by a C8/C8 double ring structure in which intrachain H-bonds are formed between NH(3) → C═O(2) and NH(2) → C═O(1), leaving NH(1) free.

In the spectra of both conformer **1B** and **1D**, the higher frequency H-bonded NH stretch has a unique shape. In **1D**, this fundamental is broadened and shaded toward higher frequency, while in **1B**, the band splits into a set of three with a spacing of 7 cm^{-1} (3401, 3408, 3415 cm^{-1}). We tentatively ascribe the peaks at 3408 and 3415 cm^{-1} in Figure 3b) to combination bands of the NH stretch with a low frequency torsion of 7 cm^{-1}. This is the same mode responsible for the Franck−Condon progression in the UVHB spectrum of this conformer (Figure 2b). The presence of such strong combination bands involving this mode in the infrared spectrum indicates either a strong coupling of this mode with the NH stretch or a large-amplitude motion involving this mode.[9]

The RIDIR spectrum of conformer **1E** (Figure 3e) shows a unique pattern, particularly in having its highest frequency NH stretch fundamental almost 20 cm^{-1} lower in frequency (3440 cm^{-1}) than the free NH stretch fundamentals for a methyl-capped (~3490−3500 cm^{-1}) or branched (~3457 cm^{-1}) free NH group. The lowest frequency band appears at 3384 cm^{-1}, near the range that is typical for a C6, C8, or C10 ring NH, but the middle band is at 3417 cm^{-1}, signaling a very weak H-bond not easily ascribable to a ring of a given size. As a result, we are unable to make a clear assignment just by looking at the pattern present in this conformer and will look to calculations (to be described in Section 3.B) to guide our assignment.

(9) Pribble, R. N.; Garrett, A. W.; Haber, K.; Zwier, T. S. *J. Chem. Phys.* **1995**, *103*, 531−544.

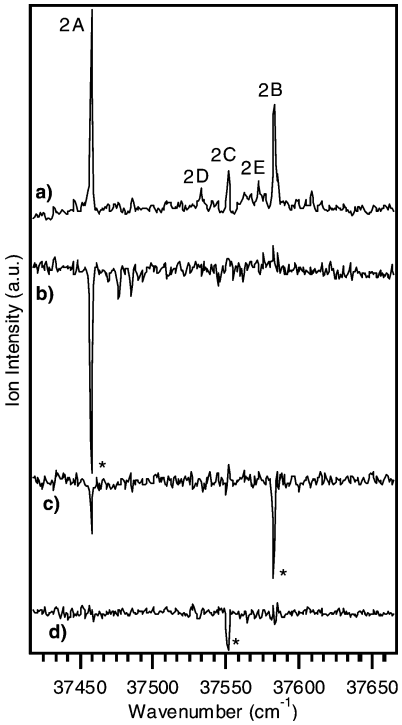

Figure 4. (a) R2PI spectrum of Ac-β^3-hAla-β^3-hPhe-NHMe (**2**). (b−d): UV hole-burning spectra of conformers 2A−C, respectively. The asterisks denote the transitions used as the hole-burn transition in each case. Labels on the R2PI spectrum show the $S_1 \leftarrow S_0$ origin transitions of all five conformers determined to be unique conformers of **2**, based on UVHB or RIDIR spectra. The small peak at the origin position of A in the UV hole-burning spectrum of B (c) is an artifact due to incomplete subtraction in the difference spectrum.

3.1.2. Ac-β^3-hAla-β^3-hPhe-NHMe (2). The top trace in Figure 4 shows the R2PI spectrum of Ac-β^3-hAla-β^3-hPhe-NHMe (**2**) in its origin region (37380−37640 cm^{-1}). As in **1**, the S_0-S_1 origin region of **2** contains several transitions that are likely candidates for origin transitions due to individual conformers. These are labeled **2A**−**E** in order of decreasing intensity in the R2PI spectrum. As in **1**, two transitions, at 37458 cm^{-1} (**2A**) and 37583 cm^{-1} (**2B**) dominate the spectrum, but the pattern of transitions and the relative spacing between them is quite different than in **1**. UV−UV hole-burning was carried out on the three most intense transitions **2A**−**C**. The resulting UVHB spectra are shown in Figure 4b−d, respectively. In each case, the origin transition dominates the hole-burning spectrum, indicating little Franck−Condon activity involving the low-frequency vibrations of the β-peptide backbone. Because of the small size of transitions **2D** and **2E**, UVHB spectra suffered from incomplete subtraction when the probe laser was tuned through the large transitions in the spectrum. As a result, it was not possible to record high-quality UVHB scans of **2D** and **2E**. However, as we will show, these transitions were ascribable to additional unique conformers by virtue of their unique infrared spectra. As a result, five conformers were resolved for **2**, the same number that were spectroscopically characterized in **1**. Table 1 lists the S_o-S_1 origins of all five conformers of **2**.

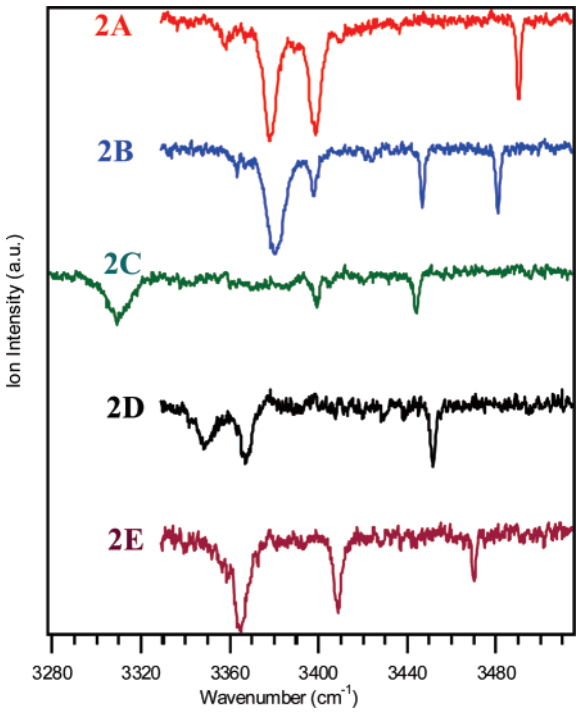

Figure 5. (2A−E) RIDIR spectra in the amide NH stretch region of conformers 2A−E of Ac-β^3-hAla-β^3-hPhe-NHMe (**2**).

Figure 5a−e shows the RIDIR spectra of conformers **2A**−**E**, respectively. As in **1**, the NH stretch fundamentals form patterns that can be used to classify, at least in a preliminary way, the H-bonding structure of the β-peptide backbone. Table 1 lists their frequencies. Conformers **2A** and **2D** are examples of structures containing two intramolecular H-bonds. The RIDIR spectrum of conformer **2A** (Figure 5a) shows two hydrogen-bonded NH stretch fundamentals around 3390 cm^{-1} and a free NH stretch fundamental at 3490 cm^{-1}, characteristic of a free methyl-capped NH stretch. Thus, conformer **2A** is a C6/C6 structure similar to that found for conformers **1B** and **1D**.

Conformer **2D** (Figure 5d) shows two hydrogen-bonded NH stretches which are shifted to lower frequency than those from **2A** by about 30 cm^{-1} (Figure 5a). The free NH stretch in **2D** is located at 3450 cm^{-1}, which is a signature of a branched free NH stretch fundamental. This pattern is consistent with a C8/C8 double ring structure for **2D**, similar to that found in conformer **1C**.

The RIDIR spectrum of conformer **2B** (Figure 5b) shows a single hydrogen-bonded fundamental at 3381 cm^{-1} and two free NH stretch fundamentals at 3447 cm^{-1} and 3487 cm^{-1}. The two free NH stretch fundamentals are separated by 40 cm^{-1} and fall close to the prototypical values for a methyl-capped and a branched-chain free NH, indicating that **2B** contains one of each. The band at 3398 cm^{-1} is believed to be a combination band that arises from the coupling of the hydrogen-bonded fundamental and a low frequency (17 cm^{-1}) torsional vibration of the molecule. The overall pattern presenting **2B** is closely analogous to that of conformer **1A**, consistent with an assignment to a structure containing a single, C10 H-bonded ring.

The RIDIR spectrum of conformer **2E** (Figure 5e) shows a pattern of NH stretch fundamentals that are quite different from the others, and in some ways reminiscent of **1E** (Figure 3e). Its two hydrogen-bonded fundamentals are at 3365 and 3409 cm^{-1}, slightly lower in frequency than the corresponding transitions in **1E**. The free NH stretch fundamental of **2E** is at 3470 cm^{-1}, a frequency mid-way between the prototypical methyl-capped (~3490 cm^{-1}) and branched (~3450 cm^{-1}) free NH stretches, making it difficult to assign the NH group responsible for it. As a result, the comparison with calculated IR frequencies and intensities will be used to guide the assignment process.

Finally, Figure 5c presents the RIDIR spectrum of conformer **2C**. There is only a single transition in the free amide NH region (3444 cm^{-1}), which appears in the region anticipated for a branched-chain free NH stretch. Two H-bonded NH stretches suggest a double ring or double ring/double acceptor structure, but the separation between the two is significantly larger than in other conformers (3309 and 3399 cm^{-1}). The band at 3399 cm^{-1} is consistent with a C6 ring or anomalous C8 ring (such as was found in **3**). A C10 H-bond would also be in this region but would require two free NH groups, counter to experiment. The 3309 cm^{-1} band is probably associated with an unusually strong C8 H-bond. A starting point, then, would be to assign **2C** to a C6/C8 or anomalous C8/C8 double ring structure. Once again, calculations will be needed to test this preliminary assignment.

3.2. Calculations: Conformational Minima, Relative Energies, and Vibrations. In order to test and refine preliminary assignments, calculations were carried out to determine the low-energy conformations of Ac-β^3-hPhe-β^3-hAla-NHMe and Ac-β^3-hAla-β^3-hPhe-NHMe and compute harmonic vibrational frequencies and IR intensities of the low-energy minima for comparison with experiment.

In order to ensure a complete search of the conformational space of **1** and **2**, two complementary approaches were taken to identifying starting geometries for structure optimizations at higher levels of theory. In one approach, a systematic grid of starting structures was generated using the dihedral angles along the β-peptide backbone (Figure 1d) based on a previous computational study of Ac-β^3-hAla-β^3-hAla-NHMe from Hofmann et al.[10−12] Alternatively, a random search was also performed using the Amber force field in the MACROMODEL[13] suite of programs. Lists of starting structures from the two methods were compared and used as the basis for structure optimizations using B3LYP density functional method[7,8] with the 6-31+G(d) basis set.[14] B3LYP and MP2 calculations were carried out with the GAUSSIAN 03 suite of programs.[15]

Figure 6 presents representative examples of the types of H-bonded conformational families observed. The structures in the top left are the prototypical C6 and C8 rings found in the study of the smaller β-peptides **3** and **4** in paper I.[5] They are reproduced here because they serve as building blocks for many of the structures found for **1** and **2**. All the low-energy minima are intrachain H-bonded structures that fall into one of three classes: single ring structures (C10, C12), double ring structures (C6/C6 and C8/C8), and double ring/double acceptor structures (C6/C8 and C8/C12).

(10) Mohle, K.; Gunther, R.; Thormann, M.; Sewald, N.; Hofmann, H. J. *Biopolymers* **1999**, *50*, 167−184.
(11) Gunther, R.; Hofmann, H. J. *Helv. Chim. Acta* **2002**, *85*, 2149−2168.
(12) Gunther, R.; Hofmann, H. J.; Kuczera, K. *J. Phys. Chem. B* **2001**, *105*, 5559−5567.
(13) Mohamadi, F.; Richards, N. G. J.; Guida, W. C.; Liskamp, R.; Lipton, M.; Caufield, C.; Chang, G.; Hendrickson, T.; Still, W. C. *J. Comput. Chem.* **1990**, *11*, 440−467.
(14) Frisch, M. J.; Pople, J. A.; Binkley, J. S. *J. Chem. Phys.* **1984**, *80*, 3265−3269.

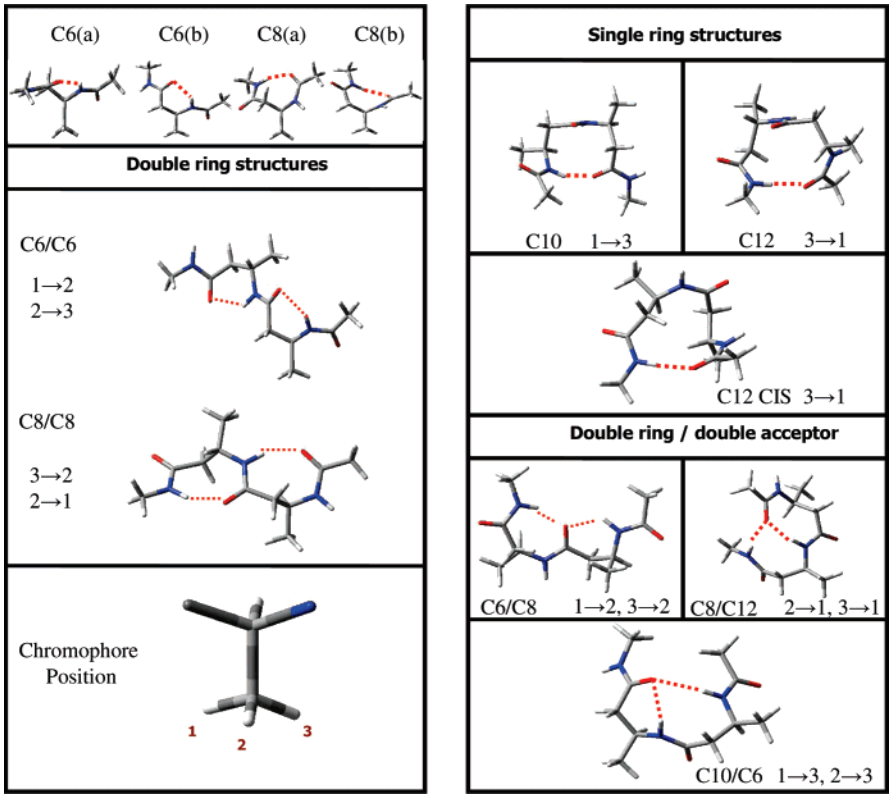

Figure 6. Representative structures of the various conformational families possible, with phenyl ring removed for clarity, grouped by H-bonding arrangement. (Left/top): C6 and C8 H-bonded rings[5] which are substructures present in double ring arrangements. (Left/center): C6/C6 and C8/C8 double ring structures. (Right/top): Single ring C10 and C12 structures, including the possibility of a C12 *cis*-amide arrangement. (Right/bottom): Double ring/double acceptor structures in which two NH groups H-bond to the same C═O group. (Left/bottom): Three possible chromophore positions for the phenylalanine side chain on the β^3 carbons. In addition to the ring labels, the number of the amide NH and the carbonyl involved in the hydrogen bonds are given in each panel (i.e., NH(no.) → C═O(no.)) using the numbering scheme from Figure 1.

In principle, single ring structures of **1** and **2** can be constructed with a C6, C8, C10, or C12 H-bonded ring. However, because C6 or C8 rings are formed between adjacent amide groups (1 → 2 and 2 → 3), it is possible to form double rings that are energetically favored over the single ring C6 or C8 structures. The same is not true for C10 or C12 rings, which link the N-terminal and C-terminal amide groups, with NH(1) → C═O(3) forming a C10 ring, and NH(3) → C═O(1) forming a C12 ring. As Figure 6 shows, C10 and C12 rings produce turns that are formal analogues of β-turns in α-peptides. In larger β-peptide chains, linking together successive C10 or C12 rings produces helical secondary structures. These helices are designated by H number (e.g., H10 or H12) to denote the number of atoms involved in the H-bonds in the helix.[16]

By contrast, C6/C6 double rings (Figure 6) possess NH(1) → C═O(2) and NH(2) → C═O(3) H-bonds that form six-membered rings on opposite sides of the β-peptide backbone, leading to extended structures. Similarly, C8/C8 double rings point the H-bonds in the opposite direction along the β-peptide chain, linking NH(3) → C═O(2) and NH(2) → C═O(1). In both C6/C6 and C8/C8 structures the C6 and C8 rings are close analogues of structures found in the smaller β-peptide (**3**) studied in adjoining publication. Recall that in **3**, three types of C6 and 5 types of C8 structures were possible.[5] Different ring types arise from different dihedral angle arrangements of the peptide chain. These arrangements are labeled a−b for C6 structures and a−e for C8 conformers. In **1** and **2**, steric hindrance with the benzyl group allows only the a and b types of C6 and C8 rings to be formed.

The final family of conformations is double ring/double acceptor, with C6/C8, C8/C12, and C10/C6 double rings possible. In these cases two NH groups from different amide units form a hydrogen bond to a single C═O group. When the central C═O(2) group plays the role of double acceptor, the NH(1) → C═O(2) H-bond forms a C6 ring, while NH(3) → C═O(2) produces a C8 ring. The double acceptor group in the C8/C12 rings (Figure 6) is the N-terminal carbonyl, C═O(1), accepting a H-bond from NH(2) to form a C8 ring and from NH(3) to form a C12 ring. Alternatively, when the C═O(3) is the double acceptor a C10/C6 arrangement is formed, where H-bond to the NH(1) forms a C10 ring while a H-bond to the NH(2) forms the C6 ring. In all these double ring/double acceptor structures, the two NH groups interact with oxygen lone-pairs on opposite sides of the acceptor oxygen atom. In both types of structures, we anticipate that the double acceptor arrangement will reduce the strength of the H-bonds formed.

The total number of conformational isomers of a given structural type is determined by the number of unique C*n* rings that can be formed (e.g., C6(a), C6(b)) and by the position of the phenyl ring. In general, the phenyl ring on the Phe side chain can take up any one of three positions (Figure 6, bottom left). In certain cases, steric effects will limit the number of positions for the phenyl ring.

(15) Frisch, M. J.; et al. *Gaussian 03*, Revision C.02; Gaussian, Inc.: Wallingford, CT, 2004.
(16) Beke, T.; Somlai, C.; Perczel, A. *J. Comput. Chem.* **2006**, *27*, 20−38.

Table 2. Calculated Energies for Conformers of Ac-β^3-hPhe-β^3-hAla-NHMe (**1**) and Ac-β^3-hAla-β^3-hPhe-NHMe (**2**) at the Indicated Level of Theory

		Ac-β^3-hPhe-β^3-hAla-NHMe (**1**)			Ac-β^3-hAla-β^3-hPhe-NHMe (**2**)		
H-bonding[a] structure	ring type and chromophore position[b]	DFT (6-31 + G*) (opt)[c]	MP2 (6-31 + G*) (sp)[d]	MP2 +ΔG[e]	DFT(6-31 + G*) (opt)[c]	MP2 (6-31 + G*) (sp)[d]	MP2 + ΔG[e]
C6/C6	a/a						
	1	0.00	0.00	0.00	0.00	0.00	0.00
	2	–	–	–	–	–	–
	3	–	–	–	6.60	5.33	1.50
	a/b						
	1	–	–	–	6.80	8.84	6.85
	2	6.07	2.75	8.47	12.91	9.63	7.27
	3	–	–	–	–	–	–
	b/a						
	1	4.90	8.45	6.49	5.42	4.49	3.48
	2	9.62	9.16	8.57	18.61	5.31	8.65
	3	–	–	–	–	–	–
	b/b						
	1	11.52	15.67	16.97	11.65	13.68	10.87
	2	15.65	14.93	13.79	17.15	8.57	8.62
	3	–	–	–	–	–	–
C8/C8	a/a						
	1	15.17	12.31	18.32	–	–	–
	2	–	–	–	21.94	12.73	20.58
	3	11.05	10.30	15.71	13.20	7.95	13.06
	a/b						
	1	–	–	–	12.48	8.40	14.22
	2	13.34	7.97	18.59	20.41	7.81	15.56
	3	7.73	0.80	10.11	12.16	1.87	11.67
C6/C8	a/a						
	1	8.65	5.55	5.81	–	–	–
	2	–	–	–	13.06	13.31	13.94
	3	–	–	–	12.43	9.91	11.67
C8/C12	a/						
	1	–	–	–	14.76	6.08	15.05
	2	–	–	–	16.43	−8.13	6.31
	3	14.01	3.51	8.33	22.48	5.89	8.62
C10/C6	/a						
	1	17.37	14.56	16.12	16.94	12.72	17.38
	2	20.31	12.05	14.83	22.77	13.94	16.24
	3	–	–	–	–	–	–
C10	a						
	1	14.21	2.97	0.83	14.80	4.27	0.75
	3	16.44	1.37	2.30	15.61	1.26	−2.03
	b						
	1	28.44	17.53	16.66	30.80	20.28	26.22
	3	30.18	15.78	16.89	31.56	16.92	21.22
C12	a						
	1	27.18	20.50	21.39	13.78	6.20	13.15
	2	25.11	13.83	19.53	–	–	–
	3	24.56	13.28	10.81	25.70	14.97	15.82

[a] Intramolecular hydrogen-bonded ring arrangements. [b] Hydrogen-bonded ring types a and b arise from different torsional angles of the peptide chain (see the adjoining publication[5] for angles). There are three possible positions (1−3) of the phenyl chromophore at the methyl-substituted β^3carbon (refer to Figure 6). [c] Zero point corrected energies of optimized structures at DFT/6-31+G* level of theory. [d] Single point, zero point corrected relative energies at MP2/6-31+G* level of theory using the DFT/6-31+G* structures. Zero point correction uses the DFT harmonic frequencies. [e] Relative free energies calculated at the stagnation temperature (510 K), using the zero point corrected MP2 single point energies to set ΔE_0.

The relative energies of all low-lying minima within the first 30 kJ/mol (at the DFT B3LYP/6-31+G* level of theory) are listed in Table 2, grouped into structures that share the same conformational family type (e.g., C6/C6). The table also includes the results of single point MP2/6-31+G* calculations. MP2[17] single point calculations using the larger aug-cc-pVDZ Dunning basis set[18−23] were also carried out on selected conformers at the B3LYP/6-31+G* optimized geometries. These are included in the Supporting Information (Table S1). Single point MP2 calculations have been determined by previous studies to give more accurate relative conformational energies than those obtained from DFT,[24−27] particularly in taking more accurate account of dispersive interactions,[28−31] which play a role in the over-all stabilization of the minima. Table 2 also includes the relative free energies of the conformational minima, computed at the preexpansion nozzle temperature (510 K) using scaled, harmonic vibrational frequencies from the DFT B3LYP/6-

(17) Moller, C.; Plesset, M. S. *Phys. Rev.* **1934**, *46*, 0618−0622.
(18) Petersson, K. A.; Dunning, T. H. *J. Chem. Phys.* **2002**, *117*, 10548.
(19) Woon, D. E.; Dunning, T. H. *J. Chem. Phys.* **1993**, *98*, 1358.
(20) Woon, D. E.; Dunning, T. H. *J. Chem. Phys.* **1994**, *100*, 2975.
(21) Woon, D. E.; Dunning, T. H. *J. Chem. Phys.* **1995**, *103*, 4572.
(22) Kendall, R. A.; Dunning, T. H.; Harrison, R. J. *J. Chem. Phys.* **1992**, *96*, 6796.
(23) Dunning, T. H. *J. Chem. Phys.* **1989**, *90*, 1007.
(24) Haber, T.; Seefeld, K.; Kleinermanns, K. *J. Phys. Chem. A* **2007**, *111*, 3038−3046.
(25) Macleod, N. A.; Simons, J. P. *Phys. Chem. Chem. Phys.* **2004**, *6*, 2878−2884.
(26) Chin, W.; Dognon, J. P.; Canuel, C.; Piuzzi, F.; Dimicoli, I.; Mons, M.; Compagnon, I.; von Helden, G.; Meijer, G. *J. Chem. Phys.* **2005**, *122*.

31+G* calculations. The relative free energies can be used to predict relative populations of the conformational isomers prior to expansion. The actual, downstream populations will depend on this initial population and the population transfer that may occur from other populated conformational minima during the expansion cooling process.[32−42]

For the majority of the conformational minima listed in Table 2, the MP2 single point and free energy corrections lead to modest changes in the relative energies (or free energies) of the conformers, particularly within each conformational family. However, there is a striking, selective stabilization of most large-ring structures (C10 single ring, C12 single ring, or C8/C12 double ring/double acceptor) relative to those forming smaller rings (C6/C6, C8/C8, and C6/C8). In particular, all but one of the eight C10 conformers listed in Table 2 are stabilized by 10−17 kJ/mol relative to C6a/C6a(1). The MP2 single point energies are responsible for the majority of this stabilization, with free energy corrections accounting for 2−5 kJ/mol of the total. The net effect is to bring the lowest energy C10 conformers of **1** and **2** into close energetic proximity to C6a/C6a(1). The C12 and C8/C12 structures are also selectively stabilized, but here the free energy correction partially compensates for the effect of dispersion, pushing the relative free energies back up in energy. In the most dramatic case, the MP2 single point calculations drop the relative energy of C8a/C12(2) relative to C6a/C6a(1) by almost 25 kJ/mol, leading to a prediction that it is the global minimum. However, this structure is entropically highly disfavored, producing a counter correction in free energy of 14.3 kJ/mol.

These results make it clear that dispersion forces play an important role that requires a description beyond B3LYP for accurate assessment of relative energies. In a case like the present one where different H-bonding arrangements are being compared, those structural families that involve a folding of the β-peptide backbone back on itself (such as what occurs in the large single rings) will have larger contributions from dispersive forces than those that are more extended, such as are found in the smaller C6/C6 and C8/C8 double rings. In the present circumstance, the single point MP2 calculations show the sign and relative magnitude of these corrections but are not able to quantitatively capture these effects. Several previous studies have pointed out the fact that B3LYP calculations underestimate dispersion,[28−31] while MP2 calculations overemphasize them.[43,44] In addition, intramolecular basis-set superposition error (BSSE) can contribute to systematic errors in the relative energies.[45−49] In order to distinguish the contribution of BSSE arising from the overlap of peptide chain atoms on top of the chromophore, single point energy calculations were carried out on select chain conformations in the absence of the benzene ring. These calculations, summarized in Table S1 of the Supporting Information, show that conformer C8a/C12(2) was the most affected by BSSE involving the phenyl ring, contributing to its apparent stabilization. Upon removal of the chromophore, the C8a/C12 chain arrangement is no longer selectively stabilized by comparison to other chain arrangements.

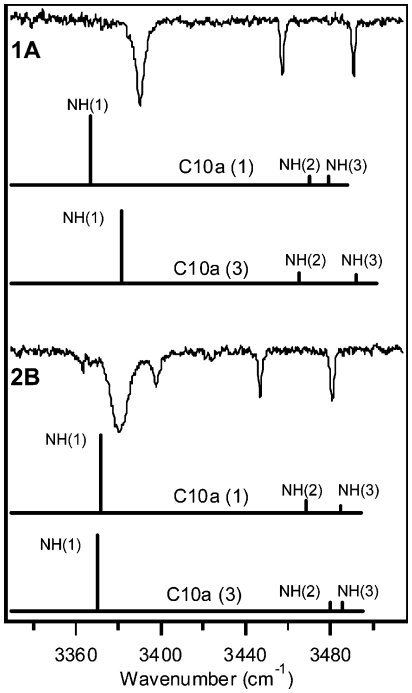

Figure 7. (1A, 2B) RIDIR spectra of conformer A of Ac-β^3-hPhe-β^3-hAla-NHMe (**1**) and conformer B of Ac-β^3-hAla-β^3-hPhe-NHMe (**2**) in the NH stretch region. The stick diagrams below the experimental spectra are calculated, scaled harmonic vibrational frequencies and infrared intensities (DFT B3LYP/6-31+G*) of representative C10 β-peptide conformational minima that best match experiment. See text for further discussion. The structures responsible for each stick spectrum are shown in Figure 12.

Harmonic vibrational frequencies and infrared intensities were calculated at the DFT B3LYP/6-31+G* level of theory for all minima of **1** and **2** included in Table 2. As already anticipated in our previous discussion, these families of structures produce very distinct NH stretch infrared spectral patterns that serve as signatures of their presence. Figures 7−11 compare the experimental RIDIR spectra for **1A**−**E** and **2A**−**E** with calculated IR spectra of structures that were found to have the best match with experiment. Figure 7 depicts the results for C10 structures, Figure 8 for C6/C6 double rings, Figure 9 for C8/C8 double rings, and Figure 10 for C6/C8 and C8/C12 double ring/double acceptor structures. Figure 11 shows calculated spectra for the

(27) Chin, W.; Piuzzi, F.; Dimicoli, I.; Mons, M. *Phys. Chem. Chem. Phys.* **2006**, *8*, 1033−1048.
(28) Zhao, Y.; Truhlar, D. G. *J. Chem. Theory Comput.* **2007**, *3*, 289−300.
(29) Wodrich, M. D.; Corminboeuf, C.; Schleyer, P. V. *Org. Lett.* **2006**, *8*, 3631−3634.
(30) van Mourik, T. *Chem. Phys.* **2004**, *304*, 317.
(31) Perezjorda, J. M.; Becke, A. D. *Chem. Phys. Lett.* **1995**, *233*, 134−137.
(32) Basu, S.; Knee, J. L. *J. Phys. Chem. A* **2001**, *105*, 5842−5848.
(33) Felder, P.; Gunthard, H. H. *Chem. Phys.* **1982**, *71*, 9−25.
(34) Fraser, G. T.; Suenram, R. D.; Lugez, C. L. *J. Phys. Chem. A* **2001**, *105*, 9859−9864.
(35) Godfrey, P. D.; Brown, R. D.; Rodgers, F. M. *J. Mol. Struct.* **1996**, *376*, 65−81.
(36) Kaczor, A.; Reva, I. D.; Proniewicz, L. M.; Fausto, R. *J. Phys. Chem. A* **2006**, *110*, 2360−2370.
(37) Kim, D.; Baer, T. *Chem. Phys.* **2000**, *256*, 251−258.
(38) Mccoustra, M. R. S.; Hippler, M.; Pfab, J. *Chem. Phys. Lett.* **1992**, *200*, 451−458.
(39) Pitts, J. D.; Knee, J. L.; Wategaonkar, S. *J. Chem. Phys.* **1999**, *110*, 3378−3388.
(40) Miller, T. F.; Clary, D. C.; Meijer, A. J. H. M. *J. Chem. Phys.* **2005**, *122*, 244323.
(41) Reva, I. D.; Stepanian, S. G.; Adamowicz, L.; Fausto, R. *Chem. Phys. Lett.* **2003**, *374*, 631−638.
(42) Ruoff, R. S.; Emilsson, T.; Chuang, C.; Klots, T. D.; Gutowsky, H. S. *J. Chem. Phys.* **1990**, *93*, 6363−6370.
(43) Wintjens, R.; Biot, C.; Rooman, M.; Lievin, J. *J. Phys. Chem. A* **2003**, *107*, 6249−6258.
(44) Hopkins, B. W.; Gregory, S. T. *Chem. Phys. Lett.* **2005**, *407*, 362−367.
(45) Levy, J. B.; Martin, N. H.; Hargittai, I.; Hargittai, M. *J. Phys. Chem. A* **1998**, *102*, 274−279.
(46) Jensen, F. *Chem. Phys. Lett.* **1996**, *261*, 633−636.
(47) Senent, M. L.; Wilson, S. *Int. J. Quantum Chem.* **2001**, *82*, 282−292.
(48) Riley, K. E.; Pavel, H. *J. Phys. Chem. A* **2007**, *2007*, 8257−8263.
(49) Holroyd, L. F.; van Mourik, T. *Chem. Phys. Lett.* **2007**, *442*, 42−46.

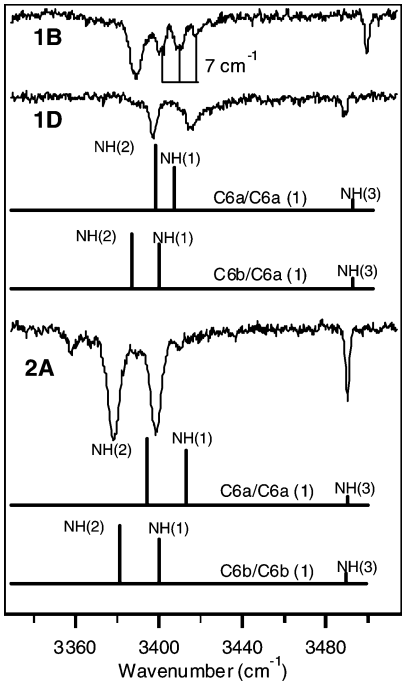

Figure 8. (1B, 1D) RIDIR spectra of conformer B and D of Ac-β^3-hPhe-β^3-hAla-NHMe (**1**) and (2A) conformer A of Ac-β^3-hAla-β^3-hPhe-NHMe (**2**), in the NH stretch region. The stick diagrams below the experimental spectra are calculated, scaled harmonic vibrational frequencies and infrared intensities (DFT B3LYP/6-31+G*) of representative C6/C6 β-peptide backbone arrangements. See text for further discussion. The structures responsible for each stick spectrum are shown in Figure 12.

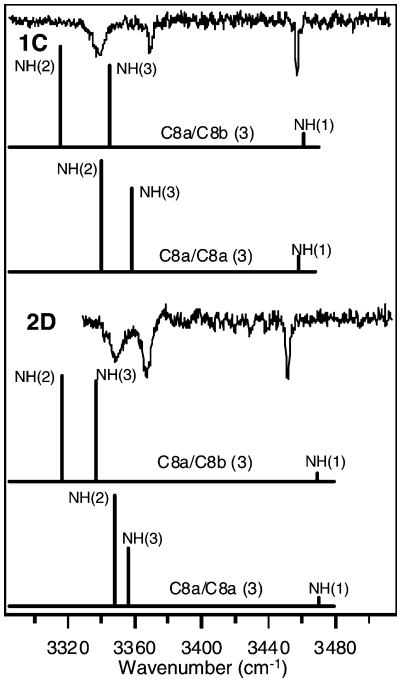

Figure 9. (1E, 2E) RIDIR spectra of conformer E of Ac-β^3-hPhe-β^3-hAla-NHMe (**1**) and conformer B of Ac-β^3-hAla-β^3-hPhe-NHMe (**2**) in the NH stretch region. The stick diagrams below the experimental spectra are calculated, scaled harmonic vibrational frequencies and infrared intensities (DFT B3LYP/6-31+G*) of representative double ring/double acceptor (e.g., C6/C8 and C8/C12). See text for further discussion. The structures responsible for each stick spectrum are shown in Figure 12.

two best matches to spectrum **2C**. The harmonic vibrational frequencies have been scaled by 0.96, the same scale factor used

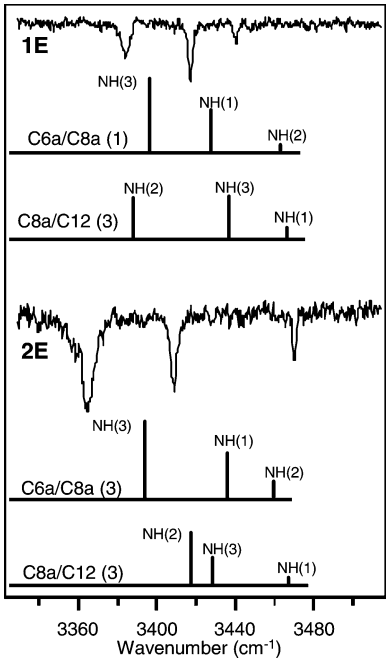

Figure 10. (1C, 2D) RIDIR spectra of conformer C of Ac-β^3-hPhe-β^3-hAla-NHMe (**1**) and conformer D of Ac-β^3-hAla-β^3-hPhe-NHMe (**2**) in the NH stretch region. The stick diagrams below the experimental spectra are calculated, scaled harmonic vibrational frequencies and infrared intensities (DFT B3LYP/6-31+G*) of representative C8/C8 β-peptide backbone arrangements. See text for further discussion. The structures responsible for each stick spectrum are shown in Figure 12.

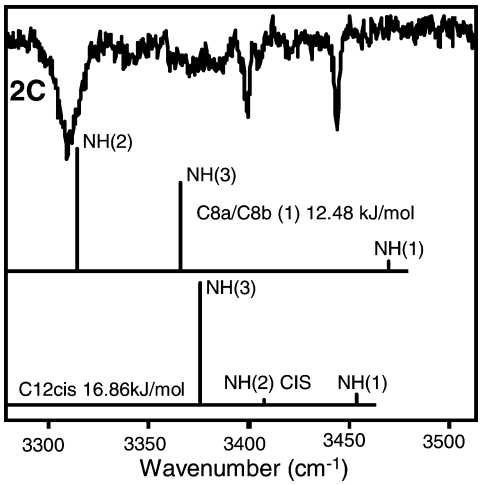

Figure 11. (2C) RIDIR spectra of conformer C of Ac-β^3-hAla-β^3-hPhe-NHMe (**2**) in the NH stretch region. The stick diagrams below the experimental spectra are calculated, scaled harmonic vibrational frequencies and infrared intensities of a representative C8/C8 and a C12 *cis*-amide β-peptide backbone arrangements.

in the preceding paper in this issue,[5] where it was chosen to match the calculated frequency of the methyl-capped free NH stretch with experiment. The structures responsible for the calculated spectra of Figures 7−11 are shown in Figure 12. The structures are labeled using the short-hand notation that gives the H-bonded rings involved and the position of the phenyl ring (1, 2, or 3, see Figure 6) The calculated vibrational frequencies and infrared intensities for all the conformers listed in Table 2 are contained in the Supporting Information.

As was discussed in the adjoining publication,[5] the calculated harmonic vibrations faithfully reproduce the experimentally observed 30−40 cm^{-1} shift between methyl-capped and branched-

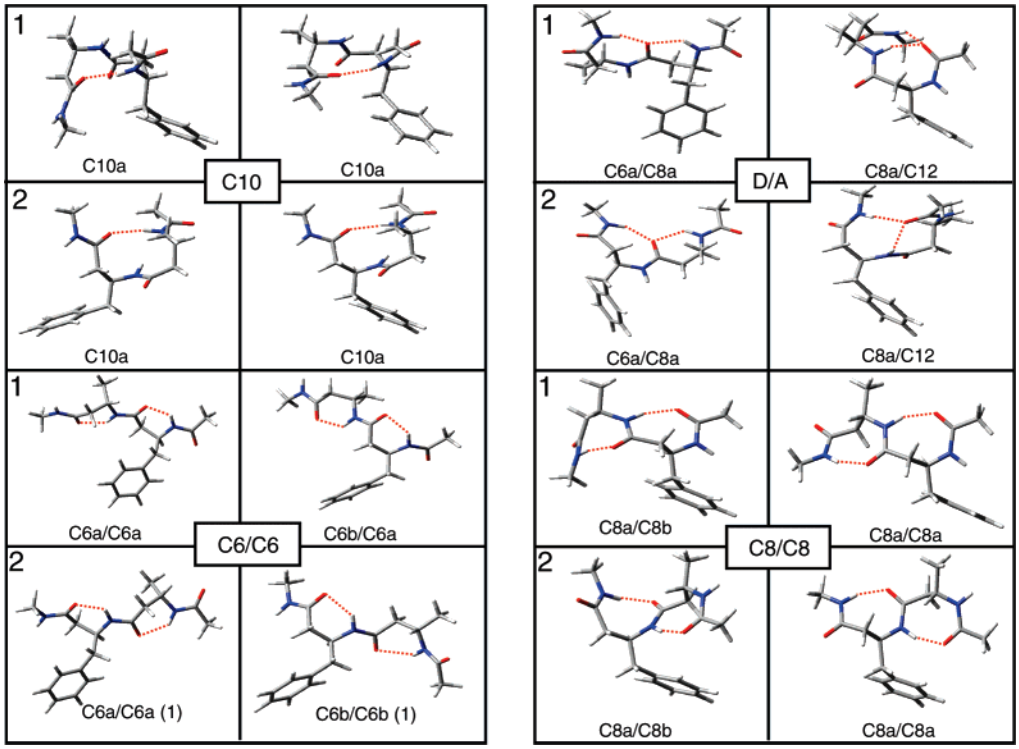

Figure 12. Optimized structures related to the calculated spectra from Figures 7−11, computed at the DFT B3LYP/6-31+G* level of theory. The numbers in the upper left-hand corner of each row indicate molecule **1** or **2**.

chain free amide NH stretch frequencies. Furthermore, the B3LYP calculations also do a remarkably good job of quantitatively predicting the positions and relative intensities of the H-bonded NH stretch fundamentals of the C10, C6/C6, and C8/C8 structures. Thus, the calculations confirm that conformers **1A** and **2B** are both single ring C10 structures (Figure 7), with one H-bonded NH stretch fundamental and two free NH stretch transitions due to branched chain (NH(2)) and methyl-capped (NH(3)) NH groups. Similarly, conformers **1B**, **1D**, and **2A** are all C6/C6 double ring structures (Figure 8), while **1C** and **2D** can be assigned with confidence to C8/C8 double ring structures (Figure 9). The calculations correctly predict the lower frequency of the C8/C8 double ring H-bonded NH stretch compared to the C6/C6 double rings.

Firm assignments for these key structural families makes it worthwhile to consider further the structural basis of the relative wavenumber positions of the S_0-S_1 origin transitions of the various conformers. The three observed C6/C6 conformers (**1B**, **1D**, and **2A**) all have S_0-S_1 origins in the 37450−37470 cm^{-1} region. In the C6/C6 double rings, the β-peptide backbone lies in a plane roughly parallel to the phenyl ring and is an extended structure. This leads to weak interaction of the β-peptide backbone with the phenyl ring, whether the phenyl ring is adjacent to amide group 1 or 2 (Figure 6). By comparison, the C8/C8 double rings **1C** and **2D** both have S_0-S_1 origins about 100 cm^{-1} higher, in the 37550−37580 cm^{-1} range. Inspection of the prototypical structures of each type in Figure 6 indicates that the amide group adjacent to the β^3 position is oriented in the opposite way relative to the phenyl group in the C8 ring compared to the C6 ring, suggesting that this amide group's orientation may be an important factor in modulating the S_0-S_1 energy separation. Indeed, the C10 rings **1A** and **2B** further confirm this hypothesis. The amide group (1) which is adjacent to the phenyl ring in **1A** is in a similar orientation to that in the C6 ring, while amide group (2) in **2B** is oriented more like a C8 structure when the phenyl ring resides there. In keeping with this, **1A** has an S_0-S_1 origin at 37456 cm^{-1}, much like that in the C6/C6 double rings, while the S_0-S_1 origin of **2B** is shifted up to 37583 cm^{-1}, a value similar to the C8/C8 double rings.

This hypothesis requires further testing. Time-dependent DFT calculations were carried out at the ground state optimized geometry to see whether the trends noted experimentally were captured by these calculations. The calculated S_0-S_1 separations covered a wider wavenumber range and did not show the clear systematic trends predicted in the preceding paragraph. TDDFT excited-state optimizations and exploration using higher levels of theory will be required to understand the structural basis of the observed trends in the shifts in the S_0-S_1 origins with conformation and phenyl ring position.

In the infrared, the match-up between experiment and theory is less satisfying for conformers **1E** and **2E**. These are the same structures that were not easily assigned based on the experimental pattern of the IR spectra in the NH stretch region (Section 3.A). Figure 10 presents calculated NH stretch vibrational frequencies and infrared intensities for representative C6/C8 and C8/C12 double ring/double acceptor structures that match reasonably well with experiment for conformer **1E** (top) and **2E** (bottom). The two H-bonded NH stretch vibrations in the C6/C8 structures (Figure 10 and Table S1) have frequencies shifted about 10 cm^{-1} up from typical C6 and C8 rings, reflecting the weakened C6 and C8 H-bonded rings that accompany the NH(3) and NH(1) groups both binding to the same carbonyl group (C═O(2)). The calculated pattern of frequencies and intensities is similar to that found in the experimental spectrum but is not quantitatively correct. This mismatch may reflect inherent limitations in B3LYP calculations in describing the two H-bonds to C═O(2), which could be unusually sensitive to electron correlation effects. In addition,

none of the calculated C6/C8 structures (Table S1) correctly predict the unusually low frequency of the experimental free NH stretch in **1E**. Given that fact, it is hard to argue unequivocally for C6/C8 over C8/C12, or vice versa, based on comparison with the calculated IR spectra. This points to the need for higher level theory on the C6/C8 and C8/C12 structures, which is currently being pursued.[50]

In this case, the wavenumber positions of the S_0-S_1 origins can provide a point of distinction between the two possible assignments. If **1E** and **2E** are both C6/C8 double ring/double acceptors, the phenyl group is in a C6 ring in **1E** and a C8 ring in **2E**. This is consistent with the 37393 cm^{-1} S_0-S_1 origin in **1E** and 37572 cm^{-1} origin in **2E**. On the contrary, the C8/C12 double ring/double acceptor would have a blue-shifted origin in **1E** (due to the C8 ring when the phenyl group is in position 1) and a red-shifted origin in **2E** (where the amide group next to phenyl position 2 has an orientation much like that in a C6 ring). This provides additional evidence supporting the C6/C8 double rings being responsible for conformers **1E** and **2E**. This assignment holds most weight despite the fact that conformer C8a/C12(2) of **2** has a single point MP2 energy that is almost 8 kJ/mol below C6a/C6a(1) (Table 2). In fact, the calculated IR spectrum of C8a/C12(2) does not match experiment even approximately (Figure 10, bottom), supporting the idea that the relative energy of this structure is artificially stabilized by the MP2 method and BSSE arising from the unusually close proximity of the β-peptide chain to the aromatic ring.

Finally, none of the 25 optimized structures of **2** possess an infrared spectrum that provides a satisfactory match with the spectrum of conformer **2C**, with its unusual pattern of NH stretch transitions. On the basis of the pattern, we had tentatively suggested either a C6/C8 double ring or an anomalous C8/C8 double ring (Section 3.A.2). In the former case, the calculated spectra never predict a large enough separation between the two H-bonded NH stretch frequencies, proposed to result from circumstances in which the H-bond in one of the hydrogen-bonded rings is strengthened at the expense of the strength of the other H-bond. In general, the double acceptor arrangement weakens both C6 and C8 H-bonded NH stretches, which is inconsistent with the spectrum of conformer **2C**. Alternatively, a C8/C8 double ring structure could form a strong and a weak H-bond if the two C8 rings were of different types. Figure 11 shows the infrared spectrum of conformer **2C** and the predicted spectra of a C8a/C8b(1) structure. Although the C8a/C8b(1) spectrum reasonably predicts the strengthening of one H-bonded stretch, it does not reproduce the unusual position or intensity of the weak band near 3400 cm^{-1}. In principle, the same unusual C8 structure that is found in Ac-β^3-hPhe-NHMe could be responsible for this weak band; however, we were not able to find stable C8/C8 minima that incorporated either the C8d(3) or C8a(2) rings proposed as possibilities in that case.

An alternative to a hydrogen bond to explain the frequency of this NH stretch is the possibility that a *cis*-amide group could be incorporated into the β-peptide chain. Such *cis*-amide structures were observed in melatonin and possessed NH stretch fundamentals near 3420 cm^{-1}.[51] In order to fit the pattern of conformer **2C**, C12 ring arrangements with a central *cis*-amide were constructed. The predicted spectra of the lowest energy C12 *cis* structure is shown in Figure 11 (bottom). As anticipated, the free *cis*-amide group is calculated to be near 3400 cm^{-1}, and its intensity is correspondingly weak due to its stature as a free NH. However, the C12 ring H-bonded stretch is much too high in frequency, providing a poor match to that part of the spectrum. As a result, further experimental and theoretical work will be required to make a firm assignment for conformer **2C**.

(50) Private comunication from Professor Kenneth D. Jordan, University of Pittsburgh, Pittsburgh, PA 15260.
(51) Florio, G. M.; Christie, R. A.; Jordan, K. D.; Zwier, T. S. *J. Am. Chem. Soc.* **2002**, *124*, 10236−10247.

4. Discussion

4.1. The Structural Diversity of β-Peptides 1 and 2. On the basis of the strong preference for C6 over C8 structures in **3** and **4**,[5] one might have thought that a single conformational family would dominate in the two longer-chain β-peptides **1** and **2** studied here. Instead, we have recorded conformation-specific IR and UV spectra for five conformers of each molecule and shown that they contain representative examples of at least four conformational families: C10, C6/C6, C8/C8, and double ring/double acceptor (probably C6/C8). This fortunate circumstance has provided the spectral signatures of all these structural families under isolated-molecule conditions, serving as benchmark data for calculations and providing an additional point of comparison for solution-phase studies.

For the most part, the observed conformations are independent of the position of the phenyl ring in the β-peptide backbone (**1** vs **2**). Beyond the four structural families represented in each, we observe an additional minor C6/C6 double ring in **1**, while in **2**, the fifth conformer (**2C**) is unassigned but seems most consistent with a distorted C8/C8 double ring.

The conformation-specific amide NH stretch infrared spectra provide a powerful diagnostic of the intramolecular H-bonding arrangement of the β-peptide backbone. Beyond this, however, we are typically not able to use these transitions to distinguish unambiguously between conformational isomers within the same family. Structures that differ either in the type of C*n* H-bonded ring (a vs b) and/or the position of the aromatic ring (1−3) differ in subtle ways that in most cases do not enable a firm assignment to a single conformation. A more detailed assessment of the differences in NH stretch transitions with ring sub-structure (e.g., C6a/C6a vs C6a/C6b) or phenyl ring position is included in the Supporting Information. There the full set of calculated infrared spectra for all low-lying conformers contained in Table 2 is included (Figures S1−S9).

The fact that the calculated infrared spectra are only modestly perturbed by ring sub-structure or phenyl ring position indicates a robustness of the characteristic spectral patterns for each conformational family, so that the frequency and intensity patterns observed here are likely to be diagnostic of local conformations taken up by other β-peptide derivatives in other environments.

Since we do not anticipate large changes in the oscillator strength or excited-state lifetimes of the various conformers of **1** and **2**, the relative intensities of the transitions in the R2PI spectra (Figures 2, 4) serve as approximate measures of the relative populations of the conformers following cooling in the expansion. On this basis, about two-thirds of the population in both **1** and **2** resides in C10 (**1A**, **2B**) and C6/C6 (**2A**, **1B**) conformers, providing evidence that these two structures are favored over others under isolated-molecule conditions. This is in keeping with the calculated relative free energies based off of MP2 single point relative energies (Table 2), which place

the lowest energy C6/C6 and C10 structures close in energy. The C6/C6 double ring is an extended "zigzag" structure, while the C10 single ring is a prototypical element of 10- or 10/12-helices which can be formed in certain longer β-peptides.[10−12,16,52]

4.2. Assignments to Specific Structures. Despite the fact that firm assignments to specific structures within a given conformational family are not possible in general, it is nevertheless worthwhile to consider the extent to which the calculations narrow the possibilities.

There are a total of four calculated C10 minima for both **1** and **2**, with the two C10a ring structures lower in energy than the two C10b rings by almost 15 kJ/mol (Table 2). As a result, the two C10a structures shown in Figure 12) are the only viable candidates for the observed C10 conformers (**1A** and **2B**), differing only in the phenyl ring position (C10a(1), C10a(3)). Of these, the relative spacing between the two free amide NH stretch fundamentals is much better reproduced by C10a(3) than C10a(1) in conformer **1A** (Figure 7, top). By analogy, it seems logical to also assign **2B** to C10a(3). However, in **2B**, the calculated spectra for C10a(1) and C10a(3) both underestimate the separation between the two free amide NH stretch fundamentals, making this assignment less secure.

By comparison, several C6/C6 double rings are close in energy to one another, differing either in the type of C6 ring (a or b) or phenyl ring position (1, 2, 3). In **1**, this close proximity is reflected in the fact that two C6/C6 conformers are observed (**1B** and **1D**). At all levels of theory in both **1** and **2**, C6a/C6a-(1) is the lowest energy C6/C6 structure (Table 2). On the basis of energy ordering, it is tempting to assign **1B** and **2A** to C6a/C6a(1); however, the match-up between calculation and experiment (Figure 8) is slightly better with other C6/C6 structures, preventing a definite assignment of **1B**, **2A**, and **1D** to specific C6/C6 conformers. The structure of C6a/C6a(1) is shown in Figure 12).

The C8/C8 conformers **1C** and **2D** are minor conformers, in keeping with their calculated free energies, which are 10−15 kJ/mol higher in energy than C6a/C6a(1). The calculated amide NH stretch IR spectra of the C8/C8 conformers (Figures S2 and S6) show some sensitivity in the splitting and relative intensities of the two H-bonded NH stretch transitions to the nature of the two C8 rings. When the two rings are of the same type (C8a/C8a or C8b/C8b), the spacing is smaller than when rings of different types are involved (C8a/C8b). Experimentally, this spacing is 30 cm^{-1} in **1C** and 19 cm^{-1}in **2D**. For **1C**, the calculated splittings are somewhat closer to experiment for C8a/C8b than for C8a/C8a; however, the differences are small enough that one cannot rule out either possibility. In **2D** (Figure 9, bottom), we can rule out C8a/C8b(1) (not shown) by virtue of its too large splitting, but three other possibilities remain. Among these, the close spacing of C8a/C8a(3) seems the best match, and this structure is the one shown in Figure 12). The MP2 single point calculations also place this C8/C8 structure as the lowest energy of the possibilities; however, the free energy correction partially counteracts this preference.

Conformers **1E** and **2E** have both been tentatively assigned to C6/C8 double ring/double acceptor structures. There is only one possibility for the former, C6a/C8a(1) (Table 2), whose structure is shown in Figure 12. In **2E**, C6a/C8a(3) and C6a/C8a(2) are both possibilities, with the latter calculated spectrum a better match with experiment, making it the preferred structure.

4.3. Conformation-Specific Spectral Signatures. On the basis of assignments of the amide NH stretch infrared spectra of the 10 conformers of **1** and **2** studied in this work, we can draw several conclusions regarding the infrared spectral signatures of the various β-peptide H-bonding arrangements. Table 1 summarizes the observed wavenumber ranges for the amide NH stretch fundamentals ascribed to C6 (3378−3415 cm^{-1}), C8 (3339−3369 cm^{-1}), and C10 (3381−3390 cm^{-1}) H-bonded rings. The C8 rings are shifted to lower frequency than all other ring sizes, with the ranges for C6 and C10 rings about 30 cm^{-1} higher and overlapping one another. In these small β-peptides, it was possible to distinguish C6 from C10 based on the number and type of free NH stretch transitions. The C6/C8 double ring/double acceptor structure **1E** has NH stretch transitions at 3417 and 3384 cm^{-1}, respectively, both out-of-range toward higher wavenumbers relative to the homo-ring C6/C6 and C8/C8 structures. This is consistent with the anticipated weakening of both H-bonds, a form of anticooperativity that accompanies formation of two H-bonds to the same acceptor site.[53]

Our results also touch on H-bond cooperativity in another sense. Recent experimental and theoretical studies[54−65] indicate that cooperative effects can play a significant role in the overall stabilization of intramolecular and intermolecular structures (e.g., helices or β sheet aggregates) held together by chains of amide−amide H-bonds. In the present case, the C6/C6 and C8/C8 structures both have an interior amide group that acts as both H-bond donor and acceptor. On the basis of the observed vibrational frequencies, there is, at most, a minor role played by cooperative strengthening of the two C6 H-bonds in C6/C6 or two C8 H-bonds in C8/C8 structures. The close correspondence between experiment and theory shown in Figures 7−11 lend confidence that the forms of the calculated NH stretch normal modes are correct. In particular, in these short β-peptides, the NH stretch fundamentals are calculated to be highly localized on a single NH group, indicating that coupling between different NH groups in the β-peptide chain is not large. The H-bonded NH stretch fundamentals in the C6/C6 double rings (3378−3415 cm^{-1}) are in the same range as in the single C6 H-bond in **3** and **4** (3398 cm^{-1}). We surmise that in short chains, a single amide group can act as both donor and acceptor with little effect on the strength of either H-bond. Longer β-peptides may build significant cooperativity,[54−60] motivating

(52) Beke, T.; Csizmadia, I. G.; Perczel, A. *J. Comput. Chem.* **2004**, *25*, 285−307.
(53) Scheiner, S. *Hydrogen Bonding: A Theoretical Prespective*; Oxford University Press: Oxford, 1997.
(54) Chen, Y. F.; Viswanathan, R.; Dannenberg, J. J. *J. Phys. Chem. B* **2007**, *111*, 8329−8334.
(55) Koch, O.; Bocola, M.; Klebe, G. *Proteins-Structure Function and Bioinformatics* **2005**, *61*, 310−317.
(56) Kobko, N.; Paraskevas, L.; del Rio, E.; Dannenberg, J. J. *J. Am. Chem. Soc.* **2001**, *123*, 4348−4349.
(57) Kobko, N.; Dannenberg, J. J. *J. Phys. Chem. A* **2003**, *107*, 6688−6697.
(58) Kobko, N.; Dannenberg, J. J. *J. Phys. Chem. A* **2003**, *107*, 10389−10395.
(59) Dannenberg, J. J.; Asensio, A.; Kobko, N. *Abstracts of Papers*; 226th National Meeting of the American Chemical Society, American Chemical Society: Washington, D.C., 2003, *226*, U330−U330.
(60) Dannenberg, J. J.; Kobko, N. *Abstracts of Papers*; 226th National Meeting of the American Chemical Society, American Chemical Society: Washington, D.C., 2003, U303−U303.
(61) Guo, H.; Karplus, M. *J. Phys. Chem.* **1992**, *96*, 7273−7287.
(62) Guo, H.; Karplus, M. *J. Phys. Chem.* **1994**, *98*, 7104−7105.
(63) Ludwig, R.; Weinhold, F.; Farrar, T. C. *J. Chem. Phys.* **1995**, *103*, 3636−3642.
(64) Ludwig, R.; Weinhold, F.; Farrar, T. C. *J. Chem. Phys.* **1997**, *107*, 499−507.
(65) Sheridan, R. P.; Lee, R. H.; Peters, N.; Allen, L. C. *Biopolymers* **1979**, *18*, 2451−2458.

single-conformation studies that extend to larger molecules. In the short β-peptides studied here, it appears that the splitting between H-bonded NH stretch fundamentals is most sensitively dependent on the type of C6 rings involved (a/a, a/b, or b/a) rather than on the number of H-bonds in which a given amide group is involved.

The corresponding comparison between C8 single ring and C8/C8 double rings is not as readily made because the observed C8 single ring conformer in **3** is a minor conformer with a structure ascribed to an unusually weak C8 H-bond (3417 cm^{-1}).[5] However, it is clear from the present study that the C8/C8 double rings have a consistently greater shift than the C6/C6 double rings.

5. Conclusion

In this study, double resonance spectroscopy has been used to record the infrared and ultraviolet spectra of single conformations of two model β-peptides Ac-β³-hPhe-β³-hAla-NHMe and Ac-β³-hAla-β³-hPhe-NHMe. The results presented here also point the way for future work. The characteristic amide NH stretch frequencies for both free amide NH and H-bonded amide NH will serve as useful benchmarks for analogous studies of longer β-peptide chains. The present results should be compared with similar studies on α/β-peptides, where the α-peptide unit changes the size of the H-bonded rings, leading to a rich set of conformational possibilities that are complementary to those studied here. The conformational diversity present in the β-peptides studied here can be modified systematically by methyl capping various NH groups, thereby removing the possibility of forming certain sized H-bonded rings and forcing the remaining possibilities to the forefront. Finally, it will be useful to study the H-bonded structures formed by β-peptide−$(H_2O)_n$ clusters, where, among other things, water molecule(s) could form bridges between amide donor and acceptor sites. The H-bonding networks so formed will reflect a balance between maintaining strong intrapeptide H-bonds and forming new structures opened up by the water molecules' ability to form multiple H-bonds, both as donor and acceptor.

Acknowledgment. E.E.B., W.H.J., and T.S.Z. gratefully acknowledge support from the U.S. National Science Foundation Experimental Physical Chemistry Program (CHE-0551075) for this work. S.H.G. and S.H.C. acknowledge support under NSF CHE-0551920. S.H.C. was supported in part by the Samsung Scholarship Foundation.

Supporting Information Available: Complete ref 15. Calculated infrared spectra, at the B3LYP/6-31+G* level of theory, for all *trans*-amide conformers of **1** and **2** within a 30 kJ/mol window as well as *cis*-amide C12 ring conformers of **2**. Single point MP2 (6-31+G* and aug-cc-pVDZ) energy calculations of selected ring structures with and without the benzene ring chromophore. This material is available free of charge via the Internet at http://pubs.acs.org.

JA078272Q